Coordination self-assembly through weak interactions in meso-dialkoxyphosphoryl-substituted zinc porphyrinates

Sergey Nefedov, Kirill Birin, Alla Bessmertnykh-Lemeune, Yulia Enakieva, Anna Sinelshchikova, Yulia Gorbunova, Aslan Tsivadze, Christine Stern, Yuanyuan Fang, Karl Kadish

ARTICLE

Coordination Self-assembly through Weak Interactions in *meso*-Dialkoxyphosphoryl-Substituted Zinc Porphyrinates

Received 00th January 20xx,
Accepted 00th January 20xx

DOI: 10.1039/x0xx00000x

Sergey E. Nefedov,[*a] Kirill P. Birin,[b] Alla Bessmertnykh-Lemeune,[*c] Yulia Y. Enakieva,[a,b] Anna A. Sinelshchikova,[b] Yulia G. Gorbunova,[a,b] Aslan Y. Tsivadze,[a,b] Christine Stern,[c] Yuanyuan Fang[d] and Karl M. Kadish[d]

The self-assembly of seven zinc 10-(dialkoxyphosphoryl)-5,15-diarylporphyrinates **Zn5–Zn11** containing different substituents at the phosphonate and aryl groups was investigated. Single crystals of **Zn5–Zn9** complexes were grown under the same conditions and analyzed by X-ray structural analysis. A supramolecular self-assembly is observed in all crystals through weak coordinative bonding of the phosphoryl group of one porphyrin molecule to the zinc(II) ion of a second porphyrin molecule. The geometry of the porphyrin macrocycle is similar in all of the studied crystals and the central zinc atom in each case adopts a distorted tetragonal pyramidal environment. However, the **Zn5–Zn7** porphyrins display a 1D polymeric structure while the **Zn8** and **Zn9** complexes exist as discrete cyclotetramers in the crystals. This data demonstrates that the non-coordinating *meso*-aryl substituents of *meso*-(dialkoxyphosphoryl)porphyrins influence their crystalline organization. A self-assembly of the **Zn5–Zn11** complexes is also observed in toluene and chloroform solutions over a large temperature range (223–323K). According to NMR studies, the associates exhibit dynamic behavior. A well-defined supramolecular aggregate of complex **Zn10** at 10^{-3} M in toluene and chloroform solutions was unambiguously characterized as a cyclotetramer **[Zn10]$_4$** by ^{1}H NMR spectroscopy at 223K. The structure of the **Zn10** association in toluene and chloroform shows a concentration dependence. When a solution of **Zn10** in toluene was diluted from 10^{-3} M to 10^{-5} M, the average number of molecules in the associated unit decreased to about two.

Introduction

Supramolecular chemistry provides ingenious strategies for the elaboration of functional systems from readily available molecular components. These methodologies have been used for the development of sensors, catalysts, energy or electron transfer systems and agents for photodynamic therapy.[1,2]
Porphyrins exhibit remarkable coordination, optical, photoelectronic and catalytic properties that can supply a target functionality to a supramolecular architecture.[3-6] Moreover, porphyrins are versatile molecular components for the design of supramolecular systems due to their topological diversity, limited conformation flexibility and their well-established synthetic chemistry that opens up a possibility to adapt the structures of molecular components and the algorithms of their assembly to a desired function or to environmental conditions. This could be one of the reasons why supramolecular systems of tetrapyrroles are widely exploited in essential processes that underlie living systems such as a photosynthesis and respiration.[7-10] Considerable recent attention has focused on the supramolecular chemistry of porphyrins and several excellent reviews have appeared recently.[11-16]
Self-assembled porphyrin systems are the simplest supramolecular architectures obviously formed by one type of porphyrin molecule.[17] The most stable and widely explored porphyrin self-assembled associates are often generated through coordinative bonding of metalloporphyrins bearing a peripheral donor site on the macrocycle. When a central metal atom is capable of axial coordination, the donor site of one molecule can ligate to the metal center of another molecule, giving a dimeric unit which still has two complementary sites suitable for coordination interactions. Both discrete and infinite dynamic systems can be generated according to this algorithm.
All metal ions displaying an axial coordination ability are suitable to prepare self-assembled porphyrin systems, with derivatives of zinc(II), magnesium(II), cobalt(III) and gallium(III) being the most widely studied.[17] The periphery of the zinc porphyrin macrocycle is usually decorated by functional moieties bearing nitrogen donor sites (pyridyl, imidazolyl, pyrazolyl or pyrimidinyl groups or aromatic amines).[18] Stability constants for zinc porphyrin binding by nitrogenous base axial ligands[19] usually lie in the range of 10^3 to 10^5. Therefore, to ensure the stability of large supramolecular assemblies in

[a.] Kurnakov Institute of General and Inorganic Chemistry, Russian Academy of Sciences - Leninsky Pr. 31 - Moscow, 119991, Russia. E-mail: snef@igic.ras.ru
[b.] Frumkin Institute of Physical Chemistry and Electrochemistry, Russian Academy of Sciences - Leninsky Pr. 31,GSP-1 - Moscow, 119071, Russia.
[c.] Institut de Chimie Moléculaire de l'Université de Bourgogne (ICMUB), Université de Bourgogne Franche-Comté (UMR CNRS 6302) - 9 Avenue Alain Savary, BP 47870 - 21078 Dijon Cedex, France. E-mail : Alla.Lemeune@u-bourgogne.fr
† Electronic Supplementary Information (ESI) available: Crystallographic information, Tables S1-S6 and Figures S1-S49. See DOI: 10.1039/x0xx00000x

solution, multiple cooperative bonding of the molecular units is often required.

Oxygen atom donors are also useful for generating supramolecular metalloporphyrin systems but these associates are obviously less stable and more difficult to investigate in comparison to those formed through metal–nitrogen coordinative bonding.[20-26] However, these supramolecular tetrapyrrole systems which are known to be generated through weak intermolecular interactions.[7,27-29] For some time, different research groups have focused on chemical modeling of the photosynthesis machinery using synthetic tetrapyrroles containing oxygen donor sites.[29-32] However, these studies are still in their infancy, in part because of difficulties encountered in growing crystals for these compounds.

Recently, phosphorylporphyrins were shown to be promising models to mimic natural supramolecular tetrapyrrole systems.[33,34] Dimers and 1D polymers formed by self-assembled *meso*-(diphenylphosphoryl)porphyrins have been characterized by X-ray structural analysis,[35,36] while only offset shifted dimers were reported for the corresponding dialkoxyphosphoryl-substituted derivatives **Zn1**–**Zn3** and **In4** (Charts 1 and 2).[37-39]

Self-assembly of these porphyrinylphosphonates is achieved through a weak axial coordination bonding of the phosphoryl group to the zinc atom of partner porphyrin molecule. *meso*-Bis(diethoxyphosphoryl)porphyrins are assembled through the same intermolecule coordination but display a 2D polymeric structure in the solid state due to the presence of two phosphoryl groups in each porphyrin molecule.[40-42] The influence of non-coordinating substituents on the structure of supramolecular aggregates was not reported.

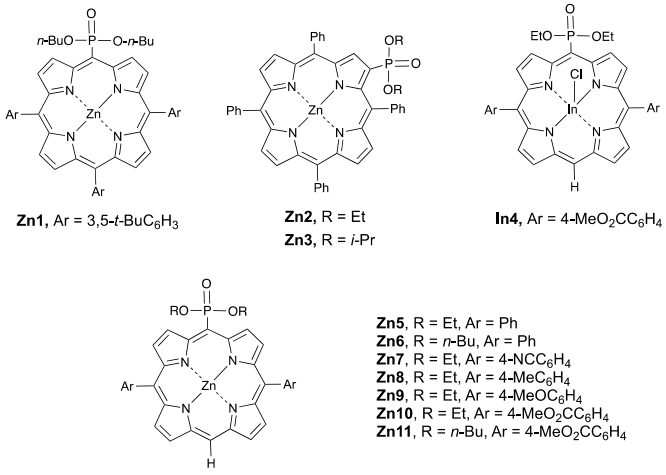

Zn1, Ar = 3,5-*t*-BuC_6H_3

Zn2, R = Et
Zn3, R = *i*-Pr

In4, Ar = 4-$MeO_2CC_6H_4$

Zn5, R = Et, Ar = Ph
Zn6, R = *n*-Bu, Ar = Ph
Zn7, R = Et, Ar = 4-NCC_6H_4
Zn8, R = Et, Ar = 4-MeC_6H_4
Zn9, R = Et, Ar = 4-$MeOC_6H_4$
Zn10, R = Et, Ar = 4-$MeO_2CC_6H_4$
Zn11, R = *n*-Bu, Ar = 4-$MeO_2CC_6H_4$

Chart 1. Structures of studied dialkoxyphosphorylporphyrins.

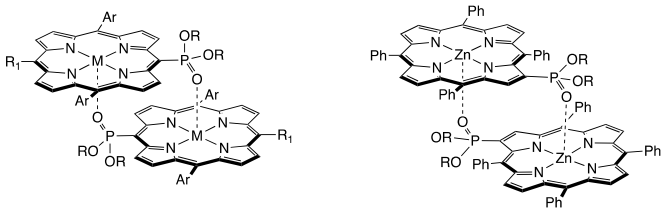

$[\mathbf{Zn1}]_2$, M = Zn, R = *n*-Bu, R_1 = Ar = 3,5-*t*-BuC_6H_3

$[\mathbf{In4}]_2$, M = InCl, R = Et, R_1 = H, Ar = 4-$MeO_2CC_6H_4$

$[\mathbf{Zn2}]_2$, R = Et

$[\mathbf{Zn3}]_2$, R = *i*-Pr

Chart 2. Structure of porphyrin dimers.

In the present paper we report a series of 10-(dialkoxyphosphoryl)-5,15-diarylporphyrins **Zn5**–**Zn9** (Chart 1) which exhibit polymeric or cyclotetrameric structures in crystals. The data on these compounds demonstrates that non-coordinating *meso*-aryl substituents influence the crystalline organization of (dialkoxyphosphoryl)porphyrins. In weakly polar solvents such as toluene or chloroform, the compounds **Zn5**–**Zn11** also form supramolecular systems which are difficult to study due to their fluxionality. However, the cyclotetramer $\mathbf{[Zn10]_4}$ can be unambiguously characterized by ^{1}H NMR spectroscopy in toluene and $CDCl_3$ at 223 K. As expected, the structure of the **Zn10** associates in solution is concentration dependent. Taken together, these results provide deeper insights into structural/organizational relationships of self-assembled porphyrin systems formed through weak coordination interactions. Preliminary studies of this work were earlier reported as a conference abstract.[43]

Results and Discussion

Synthesis

To investigate the influence of peripheral *meso*-aryl substituents on the self-assembly of phosphorylporphyrins, a series of derivatives were prepared containing both electron-rich and electron-deficient *meso*-aryl substituents while also considering steric effects of these groups. Concise and versatile methods to prepare porphyrinyl phosphonic acid derivatives have been developed in our laboratory, and the availability of these compounds opens the door to access a large number of functionalized porphyrinyl phosphonic acids and their alkyl esters.[39,40,44,45]

In this manuscript, the *meso*-(dialkoxyphosphoryl)porphyrins **Zn5**–**Zn11** were prepared from 5,15-diarylporphyrins according a two-step procedure involving their bromination and subsequent palladium-catalyzed phosphonylation by diethyl phosphite.[45] It should be noted that the reaction time of the palladium-catalyzed phosphonylation reaction must be carefully controlled because the target products, **Zn5**–**Zn11**, are slowly transformed into the corresponding monoesters of porphyrinyl phosphonic acids under the reaction conditions. A parasitic dealkylation reaction of diethyl phosphonates by triethylamine or triphenylphosphine has already been observed in the phosphonylation of halophenanthrolines.[46] Since the phosphonylation of *meso*-bromoporphyrins is

conducted in the presence of a large excess of triethylamine, a careful optimization of the reaction time using MALDI-TOF monitoring is needed to increase the yield of the target product.

Self-assembly in the solid state

Single crystals of all the **Zn5**–**Zn9** complexes were grown by a slow diffusion of hexane into 10^{-3} M solutions of the porphyrins in a $CHCl_3$/MeOH mixture (3% MeOH) and their structures were determined by X-ray structural analysis (Tables S1–S2).

Self-assembly was observed for all of the examined compounds through complementary coordination of the phosphoryl group of one porphyrin molecule to the Zn(II) center of another molecule. The crystals of complexes **Zn5**–**Zn7** consist of zig-zag coordination polymer chains. In contrast, the porphyrins **Zn8** and **Zn9** crystallized as discrete tetranuclear complexes in which four metalloporphyrin molecules are organized as a square prism missing two bases (Figure 1).

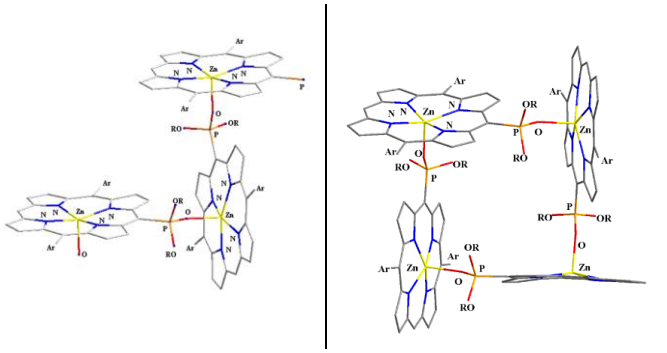

Fig.1. Schematic presentation of the spatial arrangement of porphyrin molecules in the 1D coordination polymers of (A) **Zn5**–**Zn7** and (B) the and (B) the supramolecular cyclotetramers **Zn8** and **Zn9**

Structural parameters of the porphyrin macrocycles are very similar in the studied complexes **Zn5**–**Zn9** and early reported dimers **Zn1**–**Zn3**, despite a variation of the peripheral substituents and the different arrangements of the molecules in the crystal (Tables 1 and S2). The central Zn(II) atoms adopt a distorted tetragonal pyramidal environment formed by four nitrogen atoms of the porphyrin macrocycles and one phosphoryl oxygen atom of a neighbouring molecule. The Zn–N bond distances are almost equal in all structures (2.043–2.090 Å) (Table S2). Four nitrogen atoms of the macrocycles are located in the porphyrin plane and displacement of the Zn atoms from the plane is in the range of 0.268–0.348 Å (Tables 1 and S2).

The mean N_4 planes of the coordinatively linked metalloporphyrin molecules form almost a dihedral right angle (84.8°, 88.9° and 85.8° for **Zn5**, **Zn6** and **Zn7**, respectively) (Figures 2–4 and S1–S12) while dihedral angles of the Zn(*meso*-C)P planes in two neighbouring porphyrin cores are equal to 83.8°, 86.6° and 75.3° for **Zn5**, **Zn6** and **Zn7**, respectively. The Zn–O(P) bond distances are very similar for the coordination polymers **Zn5** and **Zn7** (2.071(3) and 2.081(2) Å, respectively) and are slightly increased up to 2.113(3) Å in the complex **Zn6** due to steric hindrances induced by the bulky butoxy substituents at the phosphorus atom. It has to be noted that the Zn–O(P) bond distances in diethyl phosphonates **Zn5** and **Zn7** are very similar to those observed in dimers **Zn1**–**Zn3** which also contain the diethoxyphosphoryl group at the macrocycle periphery. Due to a similar spatial arrangement of the neighbouring porphyrin molecules in all of the studied coordination polymers, the distances between zinc atoms in these chains are quite similar and equal to 7.9396(6), 8.0633(7) and 7.8631(6) Å for **Zn5**, **Zn6** and **Zn7**, respectively. These distances are slightly larger than those observed in offset–shifted dimers **Zn1**–**Zn3**. Comparing structural parameters of the porphyrins **Zn5** and **Zn7**, we can conclude that the electron-withdrawing cyano substituent does not significantly influence

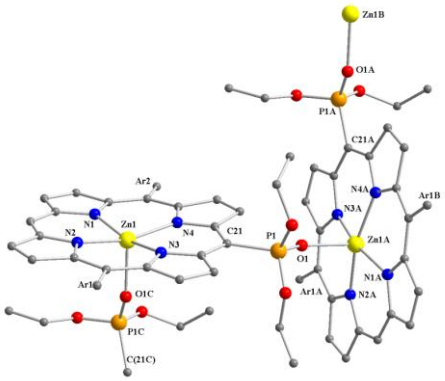

Fig. 2. Structure of coordination polymer **[Zn5]$_n$**. Hydrogen atoms, aryl **substituents and minor** disordered parts are omitted for clarity.

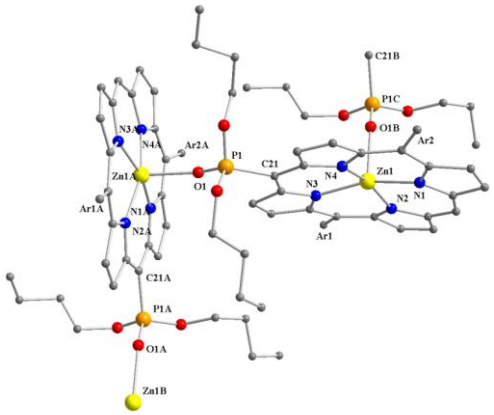

Fig. 3. Structure of coordination polymer **[Zn6]$_n$**. Hydrogen atoms, aryl substituents and minor disordered parts are omitted for clarity.

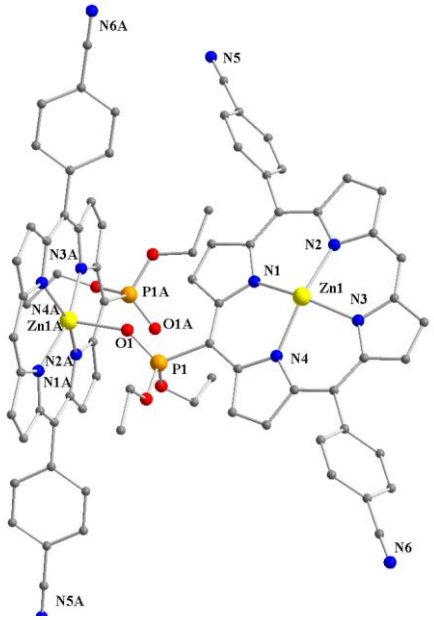

Fig. 4. Structure of coordination polymer **[Zn7]$_n$**. Hydrogen atoms, aryl substituents and minor disordered parts are omitted for clarity.

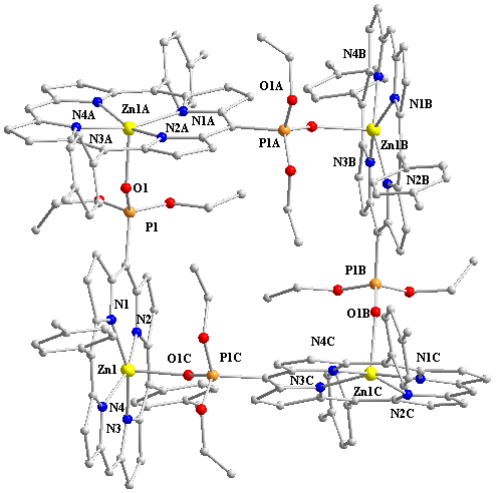

Fig. 5. Structure of cyclotetramer **[Zn8]$_4$**. Hydrogen atoms are omitted for clarity

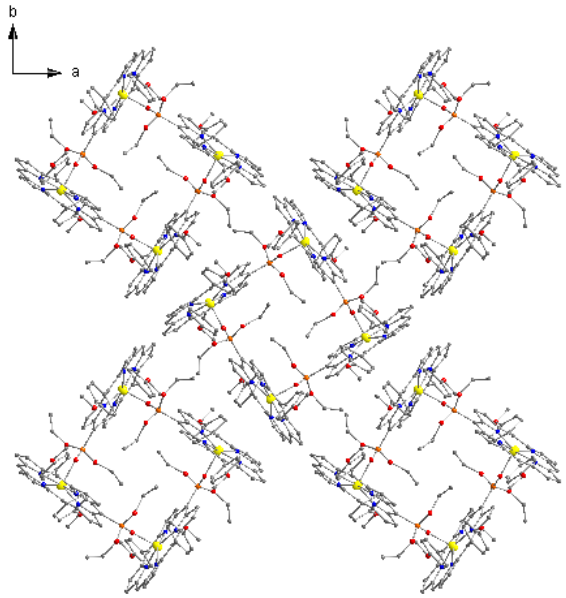

Fig. 6 Arrangement of cyclotetramers **[Zn9]$_4$** in crystals. H-atoms are omitted for clarity. Color codes: Zn – yellow, N – blue, O – red, P– orange.

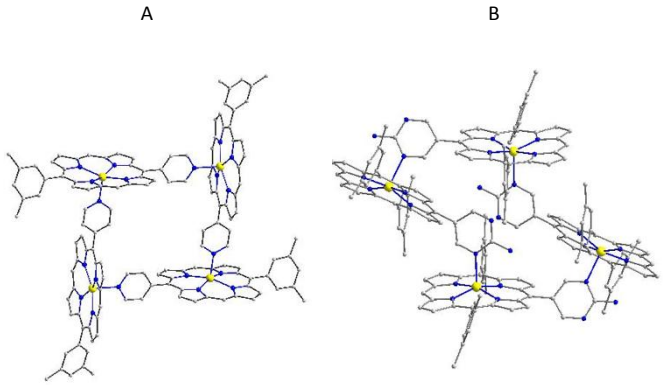

Fig. 7 Structure of complexes **Zn12**[50] (A) and **Zn14**[47] (B). Color codes: Zn-yellow, N – blue.

the self-assembly process because the Zn–O(P) and P=O bond distances and the organization of the polymer chains are similar in the two compounds. In contrast, steric effects of the aryl and phosphonate groups in the phosphorylporphyrins **Zn5–Zn7** determine the mutual arrangement of polymeric arrays in the crystals. The polymer chains of **Zn5** interact through CH···π contacts between the *para*-hydrogen atom of the phenyl substituent and a delocalized electron density of the tetrapyrrolic macrocycle (C···N = 3.416–3.461 Å and C···C = 3.800–4.018 Å) (Figure S3). Such contacts are not observed in **Zn6** and **Zn7** due to steric hindrances induced by *n*-butoxyl groups in **Zn6** or the presence of a lone electron pair at the nitrogen atom of the cyano substituent in **Zn7**. Neighbouring polymer chains in the crystals of both complexes interact through short *π–π* contacts of porphyrin macrocycles (C···N = 3.483–3.827 Å; C···C = 3.651–4.012 Å for **Zn6**; C···N = 3.445–3.831 Å; C···C = 3.555–4.021 Å for **Zn7**) (Figures S7 and S11). The distances between nearby zinc atoms of the neighbouring polymer arrays are 9.5336(9), 5.2703(9) and 7.383(9) Å for **Zn5**, **Zn6** and **Zn7**, respectively.

The porphyrins **Zn8** and **Zn9**, which bear bulky substituents at the *meso*-aryl groups, form discrete cyclic tetranuclear complexes in the crystals (Figures 5 and S13-18). These formally isostructural complexes are crystallized in the tetragonal space group P-42(1)c as compact non-porous solids. The four Zn–O distances in each of the tetramers **Zn8** and **Zn9** are equivalent and equal to 2.072(2) Å and 2.083(8) Å, respectively. These values are similar to those observed in dimers **Zn1–Zn3** and polymers **Zn5–Zn7.** One ethyl substituent of each phosphoryl group is buried at the center of the supramolecular cage while another is located on the outside of the cavity. The mean N_4 planes of the macrocycles of opposite porphyrin molecules are not parallel and form dihedral angles of 29.6 ° and 22.7° in **Zn8** and **Zn9**, respectively. The angles between the planes of adjacent porphyrins are similar in each of two structures and equal to 86.3 ° and 87.8 ° for **Zn8** and **Zn9**, respectively. The four zinc atoms of the tetramers **Zn8** and **Zn9** are situated in almost the same plane (deviation ± 0.279 and ± 0.185 Å for **Zn8** and **Zn9,** respectively) and form a square with sides of 8.042 and 8.053 Å, respectively, and diagonals of 11.346 and 11.376 Å, respectively. It has to be noted that the geometry of the phosphoryl group induces a significant deviation from the right angle for the dihedral angle between the mean N_4 plane and the plane formed by four zinc atoms (75.2 and 78.6 Å for **Zn8** and **Zn9**, respectively). A large internal space limited by porphyrin molecules is filled by four ethoxy groups belonging to four porphyrin molecules.

The individual units of the tetranuclear fragments **[Zn8]$_4$** and **[Zn9]$_4$** are interlocked along the [001] crystallographic direction into infinite chains in which the tetramer units are parallel and have numerous CH–π contacts of *ortho*-, *meta*- and *para*-hydrogen atoms of phenyl substituents with the π-system of the porphyrin macrocycle (C···N = 3.567–3.600 Å, C···C = 3.720–3.909 Å; C···N = 3.477–3.920 Å, C···C = 3.714–3.913 Å for **Zn8** and **Zn9,** respectively). The smallest angle defined by the diagonals in squares formed by four zinc atoms

in two neighbouring columns (Figure S19) are equal to 24.7 ° and 24.9 ° for **Zn8** and **Zn9,** respectively (Figures 6, S15 and S18).

To our knowledge, supramolecular tetramerization of *meso*-phosphorylporphyrins through weak Zn–O(P) binding has not previously been reported but tetrameric associates of complementary metalloporphyrins have been described. For example, according to NMR, UV-vis and electrochemical data, Zn(II),[47] Ru(II)[48] and Rh(III)[49] *meso*-(4'-pyridyl)porphyrinates **M12** (M = Zn(II), Ru(II), Rh(III)) containing a strong nitrogen donor pyridine group at the periphery of the macrocycle exhibit a tetrameric structure in chlorinated solvents. To prove a perpendicular arrangement of the neighbouring porphyrin macrocycles in these tetramers, complexes of **[Zn12]$_4$**[47] and **[Ru12]$_4$**[48] were characterized by X-ray structural analysis (Figure 7A). Another spatial arrangement of porphyrin molecules was reported for tetramers of zinc *meso*-(2'-aminopyrimidin-5'-yl)porphyrinate **Zn13**[50] and zinc *meso*-(3'-pyridyl)porphyrinate **Zn14**[47] in which the nitrogen lone pairs lie out of the plane of the macrocycle. In these associates, the porphyrin macrocycles form small dihedral angles that leads to an inequivalence in the spatial arrangement of peripheral heteroaromatic substituents in each of the two neighbouring porphyrin molecules (Figure 7B).

The structures of the *meso*-phosphorylporphyrins **Zn8** and **Zn9** are similar to that of the (4'-pyridyl)porphyrinates **M12** (M = Zn(II), Ru(II)). However, in the **M12** complexes, the neighbouring porphyrin molecules lie in the plane of symmetry of the partner macrocycle. A considerable distortion from this arrangement is observed in the tetramers **Zn8** and **Zn9** as a result of the geometry of the phosphoryl donor group (Figure 5). It should be noted that organization of the supramolecular units formed by each three consecutive porphyrin molecules is similar in both the coordination polymers **Zn5**–**Zn7** and the cyclotetramers **Zn8** and **Zn9** (Figure 1). The only important difference between the two groups is a mutual orientation of the phosphoryl groups in the first and the third porphyrin molecules. Accordingly, the three-molecule unit which is pre-organized for polymer formation can be transformed into the structural fragment of the tetrameric complex by a simple rotation of the porphyrin core around the axis of the Zn–O bond in one of the end molecules.

The size of the substituent at the aryl group appears to be critical in determining organization of the 10-(dialkoxyphosphoryl)-5,15-diarylporphyrins **Zn5**–**Zn9** in the crystals. The porphyrins containing *meso*-phenyl and 4-cyanophenyl groups display 1D polymeric structures while the bulkier derivatives of **Zn8** and **Zn9** tend to form discrete supramolecular complexes. The increase in the number of aryl substituents up to three or four in porphyrinylphosphonates **Zn1**–**Zn3** favours crystallization of dimers.

Noteworthy, the structures of 5-phosphoryl-10,15,20-triarylporphyrin **Zn1** and the 2-phosphoryl-5,10,15,20-tetraarylporphyrins **Zn2** and **Zn3** were reported earlier.[37,38] All of these complexes exist as shifted cofacial dimers in the solid state and in solution (Chart 2). Such supramolecular organization may also be favoured by steric hindrance induced by three or four bulky *meso*-aryl substituents at the periphery of the macrocycle and also demonstrate the capacity of the non-coordinating peripheral functional groups to influence the crystalline self-assembly of the dialkoxyphosphorylporphyrins.

Unfortunately, all attempts to prepare single crystals of **Zn10** and **Zn11** failed when crystalizing the compounds under the same conditions as those which were used for growing the crystals of **Zn5**–**Zn9** (10^{-3} M solution in $CHCl_3$/MeOH mixture (3% MeOH)).

Self-assembly in solutions

NMR studies. Taking into account the molecular topology of **Zn5**–**Zn11** in which only one phosphoryl donor group is present at the periphery of the macrocycle, their most probable associates in solution may be a zig-zag polymer, a shifted cofacial dimer and/or a cyclotetramer as shown in Chart 2 and

Figure 1. The different spatial arrangement of aromatic fragments in these self-assembled systems should provoke unambiguous signatures in their ^{1}H NMR spectra due to ring-current effects. For example, two ethyl groups of the coordinated phosphonate group in the coordination polymers and dimers occupy virtually equal positions with respect to the partner porphyrin macrocycle and lie in the ring-current shielding zone. A single set of resonances is expected for these two groups in both structures due to the molecular symmetry of these species. In contrast, signals of two inequivalent ethyl groups should be observed in the spectrum of the cyclotetramer

Table 1. Selected bond distances and angles of (dialkoxyphosphoryl)porphyrins **Zn1**—**Zn3** and **Zn5**—**Zn9**.

Compound	**[Zn1]$_2$**	**[Zn2]$_2$**	**[Zn3]$_2$**	**[Zn5]$_n$**	**[Zn6]$_n$**	**[Zn7]$_n$**	**[Zn8]$_4$**	**[Zn9]$_4$**
Reference	37	38	38	this work	this work	this work	this work	this work
Zn(1)–O(1) (Å)	2.102(3)	2.086(7)	2.098(4)	2.071(3)	2.113(3)	2.081(2)	2.072(2)	2.083(8)
P(1)–O(1) (Å)	1.478(3)	1.460(7)	1.474(4)	1.469(3)	1.475(3)	1.468(3)	1.469(2)	1.456(9)
deviation of Zn from N_4 plane (Å)	0.331	0.317	0.348	0.268	0.282	0.333	0.305	0.311
max deviation of C from N_4 plane (Å)	0.0086	0.0006	0.028	0.0146	0.0283	0.0134	0.0101	0.0003
planes N_4–N_4 dihedral angle (º)	0	0	0	84.8	88.9	85.8	86.3	87.8
Zn···Zn (Å)	6.253	7.187	7.336	7.939	8.063	7.863	8.042	8.053
planes N_4–*meso*-CPO[a] dihedral angle (º)	26.7	25.0	15.7	8.9	7.4	34.9	10.3	9.3

[a] *meso*-C is the carbon atom bearing the phosphonate substituent (for example, C_{21} for compound **Zn5** shown in Figure 2).

because these groups differ whether they are directed inside or outside the cavity formed by four porphyrin molecules. The internal ethyl groups lie in proximity to two partner porphyrin macrocycles and consequently their resonances should be strongly upfield shifted in comparison with signals of the outer ethyl groups and the corresponding protons of other associates.

^{1}H NMR spectra of the porphyrins **Zn5**–**Zn11** recorded at room temperature in $CDCl_3$/MeOH-d_4 (2:1) reveal all expected signals of monomeric species. In order to gain insight into structures of the **Zn5**–**Zn11** associates in solution, variable-temperature NMR studies were carried out in both weakly coordinating solvents, toluene-d_8 (223–373K) and $CDCl_3$ (223–323K).

Distinct signals were observed in the aromatic region of the spectra for **Zn5**–**Zn11** at 373K in toluene-d_8, and their positions and coupling patterns were similar to those of the monomeric species **Zn5**–**Zn11** (Figures 8 and S20-S26). The only exception was the signal of the β-protons adjacent to the *meso*-phosphonate group. This signal was slightly broadened in all spectra and shifted upfield to δ = 9.5 ppm in the spectrum of **Zn10**. This can be interpreted by assuming a coordination self-assembly process because these protons occupy the nearest position relative to the partner porphyrin macrocycle in the associates and should exhibit a higher sensitivity to self-assembly compared to other protons of the macrocycle. In agreement with this assumption, signals of the OCH_2 groups are also broadened and shifted upfield (δ = 3.0 ppm) with respect to the corresponding signals of the monomer species in $CDCl_3$/MeOH-d_4 (δ = 4.5–4.3 ppm). Similar broadening and upfield shifts of these signals were observed in the spectra of **Zn5**–**Zn11** in $CDCl_3$ at 323 K (Figures S27-S33).

All of the compounds display poorly-resolved proton signals at ambient temperature, both in $CDCl_3$ and in toluene-d_8, revealing a slow exchange between monomeric and associated species (Figures 8 and S20–S33). A decrease of the temperature to 223 K resulted in improvement of the spectrum resolution. Under these experimental conditions, the resonances are still broadened in both solvents for all compounds, but the spectrum of **Zn10** can be used for detailed structural analysis.

A set of resonances observed for **Zn10** in toluene-*d8* is complicated and differs significantly from that of the monomeric species (Figure 8). Analysis of the signals corresponding to the tetrapyrrolic macrocycle have revealed that only one associate exists in the studied solution. The most important features of the spectrum are a single signal of the*meso*-proton and strong upfield shifts for resonances of the phosphonate substituent compared to both the monomer and the earlier-reported dimeric species **Zn1**–**Zn3**.[38] The diastereotopic protons of two OCH_2 groups appear in δ regions of –2.0 to –0.5 and 0 to 1.5 ppm as four multiplets that indicate an inequivalence of the ethoxy groups at the phosphorous atom caused by their orientation with respect to the partner porphyrin molecule.

The chemical shift of the *meso*-proton resonance is virtually independent of temperature, while signals of the β-pyrrolic protons are changed throughout the whole temperature range. Three characteristic upfield-shifted doublets are observed at 5.32, 7.42 and 7.54 ppm at 223 K. Using the values of the coupling constants, these and other non-overlapping resonances of the aromatic protons can be easily separated into two groups corresponding to the aryl substituents (J = 7.5–7.8 Hz) and the tetrapyrrole macrocycle (J = 4.5–4.6 Hz). However, ^{1}H–^{1}H COSY and ^{1}H–^{1}H ROESY experiments were needed for unambiguous assignment of all proton signals (Figures S34 and S35). The labelling scheme of the protons and their assignments are summarized in Table 2.

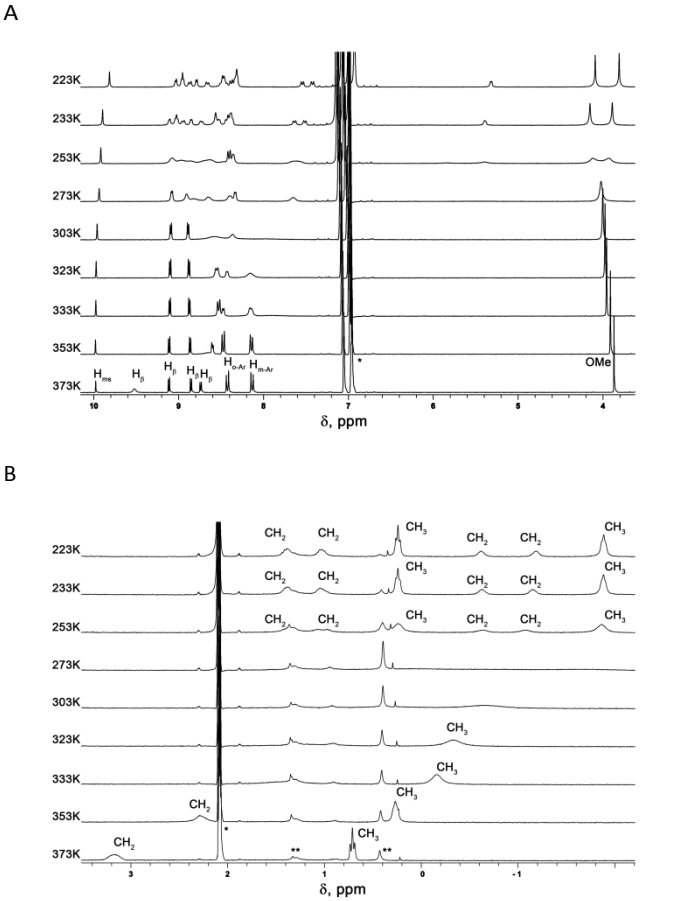

Fig. 8 Variable-temperature ^{1}H NMR spectra (aromatic (A) and aliphatic (B) regions) of porphyrin **Zn10** in toluene-*d8* (10^{-3} M). Residual signals of the solvent and signals of impurities are marked as * and **, respectively.

According to cross-peaks in the COSY map, the β-pyrrolic protons appear as four pairs of doublets that indicate a complete desymmetrization of the porphyrin macrocycle.

Among different supramolecular associates which can be expected for **Zn10** in solution (Chart 2 and Figure 1), only the structure of the cyclotetramer **[Zn10]$_4$** corresponds to such a complicated spectral pattern due to the low symmetry environment of the porphyrin macrocycle in this cyclotetramer. This is analogous to what is seen for the

complexes **Zn8** and **Zn9** in the solid state (Figures 5 and 6). In agreement with this structure, the total intensity of the aromatic protons of the *meso*-aryl substituents is distributed between eight signals while that of the methoxy groups is shared between two singlets. Through-space correlations were used to attribute the upfield-shifted β-pyrrolic protons H^2 and H^3 and the signals of the *ortho*-protons of the *meso*-aryl group adjacent to these protons. In turn, the cross peaks involving *meso*-protons of the porphyrin macrocycle were useful to assign the protons H^{13} and H^{17} of the macrocycle.

Exchange cross peaks were also observed in the ROESY spectrum at 223 K between two signals of methoxy protons, as well as corresponding signals of the internal and outer ethyl groups, showing a fluxional behavior of the supramolecular associate **[Zn10]$_4$** (Figure S47).

The variable-temperature NMR spectra of **Zn10** were also recorded after addition of small amounts (20 μL) of methanol-*d4* to a 10^{-3} M solution of this compound in toluene-d_8 (Figure S36). Under these experimental conditions, a set of resonances of the monomeric species remains unchanged over a large temperature range, although a slight broadening was observed at low temperatures. Thus, the axial coordination of methanol molecules to zinc centers on the porphyrin cores suppressed the self-assembly of complex **Zn10** in toluene-d_8 solution.

The spectrum of complex **Zn10** recorded in $CDCl_3$ at 223 K is very similar to that obtained in toluene-d_8. Characteristic signals of the ethoxy groups and ß-pyrrolic protons of the cyclotetramer **[Zn10]$_4$** are clearly observed and their intensities are in agreement with the hypothesis that a cyclotetramer is the major species in the examined solutions (Figure S44).

The spectra of **Zn5** and **Zn7–Zn9** in toluene-d_8 are more complicated and poorly resolved, even at 223 K. The intensities of all observed signals are low due to limited solubility and fluxional behavior of the studied compounds. Characteristic signals of the cyclotetramer, namely upfield-shifted signals of the phosphonate substituents and one of the β-pyrrolic protons, are observed at δ = –2.5 to 0 and δ = 5.0 to 5.5 ppm, respectively. However, the ratio of proton intensities of the inner and outer ethyl groups significantly differs from 1:1, and additional signals are present in the aromatic region. Accordingly, we assumed that several associates exist in these studied solutions, even at 223 K, but a complete structural analysis of these mixtures was not possible.

It also has to be noted that the spectra of **Zn5** and **Zn7** display a polymeric structure in the crystal which is similar to that of the complexes **Zn8** and **Zn9** which form discrete cyclotetramers in the solid state.

Table 2. Labeling scheme and assignment of resonances in ^{1}H NMR spectrum of cyclotetramer **[Zn-10]$_4$**.

δ (ppm)	Intensity	Multiplicity, *J* (Hz)	Assignment
-1.96	3H	br s	Me^i
-1.26	1H	br s	CH_2^i
-0.69	1H	br s	CH_2^i
0.17	3H	t, *J* = 6.6	Me^o
0.96	1H	br s	CH_2^o
1.31	1H	br s	CH_2^o
3.81	3H	s	OMe(2)
4.90	3H	s	OMe(1)
5.32	1H	d, *J* = 4.6	H^3
7.42	1H	d, *J* = 7.8	$H_{o(1)}$
7.54	1H	d, *J* = 7.8	$H_{o(2)}$
8.27-8.35	4H	m	H^2+H^8+ $H_{m(2)}$+$H_{m(1)}$
8.38	1H	d, *J* = 8.0	$H_{m(1)}$
8.41-8.54	2H	m	H^7+$H_{o(1)}$
8.66	1H	d, *J* = 8.2	$H_{o(2)}$
8.79	1H	d, *J* = 4.2	H^{18}
8.87	1H	d, *J* = 8.0	$H_{m2'}$
8.92-9.00	2H	m	H^{12}+H^{17}
9.03	1H	d, *J* = 4.1	H^{13}
9.81	1H	s	H_{ms}

The labelling scheme for the phosphonate substituent (A) and aromatic protons (B) is shown below.

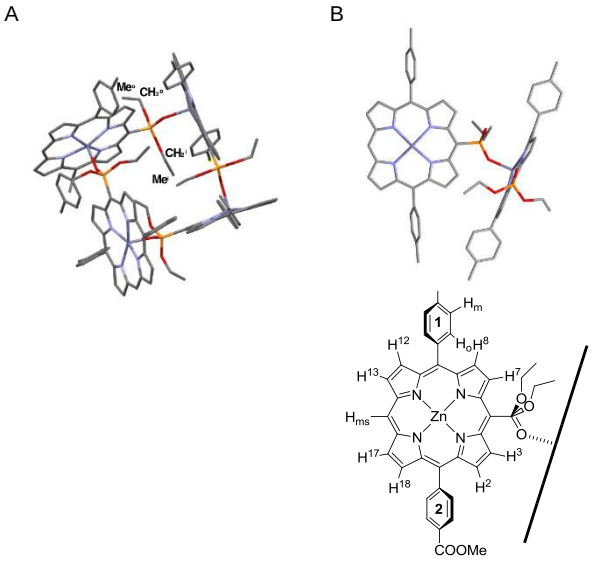

The variable-temperature NMR spectra of *meso*-(di-*n*-butoxyphosphoryl)porphyrins **Zn6** and **Zn11** in toluene-d_8 and $CDCl_3$ are also significantly broadened, and characteristic signals of the cyclotetramers are not observed for these compounds. It seems that the complexes bearing bulky butyl groups at the phosphorous atom form linear oligomers in the studied solutions.

Variable temperature ^{31}P NMR spectra were also obtained for **Zn5–Zn11** in $CDCl_3$ and toluene-d_8. In each spectrum, only a single sharp phosphorus signal was observed in the 22–24 ppm

region which was shifted upfield by *ca*. 2 ppm upon lowering of the temperature (Figure S37). These data are in agreement with the formation of axially-associated species,[37] but unfortunately are useless for structural analysis.

Finally, it should be pointed out that the ^{1}H NMR characterization of the cyclotetramer **[Zn10]$_4$** in toluene-d_8 and $CDCl_3$ at 223 K shows the largest discrete porphyrin associate formed through metal–oxygen coordinative bonding in solution. The kinetic inertness of this large tetrameric complex can be explained by a restriction of conformational freedom in this sterically hindered porphyrin cage.

UV-vis studies of Zn10. The self-assembly of **Zn10** in more dilute solutions (5 x 10^{-6} to 5 x 10^{-3} M) was also investigated by ground state electronic absorption spectroscopy. Variable-temperature UV-visible experiments were first performed in toluene (273–370 K) and chloroform (273–330 K). For a 10^{-4} M toluene solution of **Zn10**, notable hypsochromic shifts or increase of band intensities were observed for the Q bands at 551 and 584 nm (4 and 5 nm, respectively) when the temperature was raised to 323 K (Figure 9). Such shifts of absorption bands would be typical for self-assembled porphyrin systems.[51] The spectrum recorded at 323 K was attributed to monomeric **Zn10** because at higher temperatures the wavelength maxima of the Q bands remained constant. The fact that reproducible spectra were obtained when heating/cooling cycles were repeated 3 times confirms the absence of a thermal decomposition for the studied porphyrin. Similar, but smaller, hypsochromic shifts of the Q bands were observed when a chloroform solution of **Zn10** was heated to 330 K (Figure S38).

In order to prove this hypothesis, a titration of **Zn10** by methanol in toluene was performed, with subsequent heating of the resulting solution (Figures S39 and S40). The addition of methanol to a self-assembled associate formed through Zn···O(P) coordinative bonding should lead to replacement of the phosphonate group by a methanol molecule in the coordination sphere of the zinc center as was discussed above. Thus, if the spectral changes of **Zn10** in toluene at 273–323 K are induced by self-assembly, similar changes should be observed at constant temperature after addition of methanol. Indeed, a gradual bathochromic shift of wavelengths (up to 4–5 nm) with the simultaneous increase of band intensities was observed for the Q bands after the stepwise addition of 80 μL of methanol to the studied solution at 298 K (Figure S39).

Moreover, a variable-temperature study of the final solution in the 283–330 K temperature range revealed that the increase of temperature caused only a small decrease of the Q-band intensities without any significant shift of their maxima (Figure S40). This is in contrast to what was observed for the solution of complex **Zn10** in dry toluene over this temperature range.

Similar bathochromic shifts of the Q bands occurred when a solution of **Zn10** in toluene was titrated with PPh_3O, and this results from a replacement of the phosphonate group by this ligand, leading to the formation of a monomer complex (Figure S41).

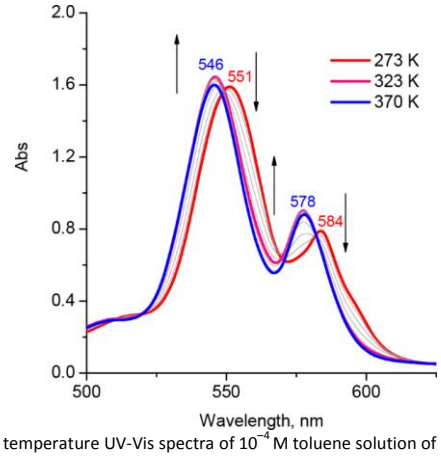

Fig. 9 Variable temperature UV-Vis spectra of 10^{-4} M toluene solution of complex **Zn10**.

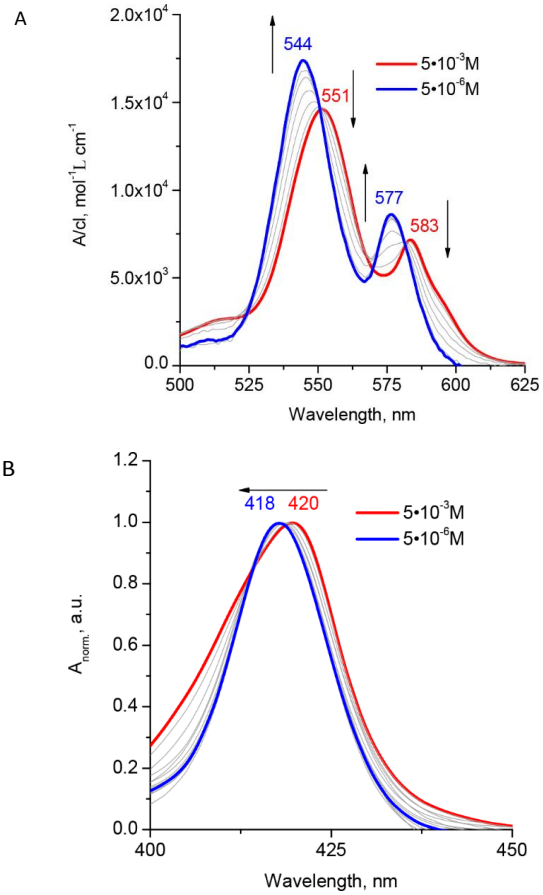

Fig. 10 Concentration dependent UV-Vis spectra of complex **Zn10** in toluene at 298 K (c = 5 x 10^{-3} to 5 x 10^{-6} M) in (A) the Q band region and (B) the Soret band region.

The concentration dependence of the absorption bands for **Zn10** in toluene at 298 K is also in accordance with the formation of supramolecular associates. Significant hypsochromic shifts with a simultaneous increase in intensity of the two Q bands (7 and 6 nm) were observed when the solution was gradually diluted from 5 x 10^{-3} to 5 x 10^{-6} M (Figure 10A). Noteworthy, the Soret band broadened significantly and shifted to shorter wavelengths in these experiments (Figure 10B). However, a splitting of this band, which is a characteristic feature for solutions of dimeric

[Zn1]$_2$[37] and other shifted cofacial porphyrin dimers[52,53] in weakly polar solvents, was not observed. The UV-vis spectrum of the complex **Zn10** in chloroform displays similar, but less significant, concentration-dependent absorption changes (Figure S42).

The average number of chromophore molecules in the supramolecular associates of **Zn10** was estimated in toluene at 298 K using the method developed by Mataga (see Experimental Section).[54] The calculated values obtained using the absorption bands at 544 and 577 nm were about 2, which indicates that the tetranuclear complex observed by ^{1}H NMR spectroscopy at 223 K in 10^{-3} M toluene solution dissociates in more dilute solutions, generating smaller supramolecular associates.

Thus, the dilution of a 5×10^{-3} M toluene solution of **Zn10** to 5×10^{-6} M induces a change in the composition of the self-assembled species and leads to generation of smaller supramolecular associates.

Electrochemical studies of Zn10. The coordination self-assembly of porphyrinylphosphonate diesters in non-aqueous media could be electrochemically observed by a splitting of the first oxidation or first reduction potentials.[34, 41, 52, 53] However, the electrochemical behavior of these porphyrins is strongly dependent on the electronic effects of peripheral substituents at the macrocycle, and commonly they exhibit typical electrochemical properties of porphyrin monomers.[41]

Zn10 exhibits a tetrameric structure in 10^{-3} M solution in chlorinated solvents and we briefly investigated its electrochemical behavior, focusing on the electrochemical signatures of this unusual aggregate. The compound was examined by cyclic voltammetry in three non-aqueous solvents (PhCN, CH_2Cl_2 and Py) containing 0.1 M TBAP (Figure 11). In each solvent, the electrochemistry of **Zn10** can be described in terms of the known electrochemistry for electron-deficient *meso*-tetraarylporphyrin derivatives, namely easier reductions and harder oxidations.[57] Two one-electron oxidations are seen in the voltammograms corresponding to the formation of the π-

cation radical and the dication. Three one-electron reductions observed in CH_2Cl_2 and PhCN, these processes being assigned to the stepwise formation of π-anion radicals and dianions followed by reduction of an *in-situ* generated phlorin anion radical.[57] The generation of a phlorin anion radical after the second reduction of **Zn10** was confirmed by electrochemical data in the more basic pyridine solvent. As expected, the amount of phlorin formation was decreased to almost zero in pyridine and only two one-electron reductions are observed in the cyclic voltammogram (Figure 11c).

The effects of substituents on redox potentials can generally be quantitated by the linear free energy relationship $E_{1/2} = \Sigma\sigma\rho$, where $E_{1/2}$ is the half-wave potential for each redox process of the compound, σ is the Hammett substituent constant and ρ, measured in volts, represents the sensitivity of the given redox reaction to the change of substituents.[58,59] Half-wave potentials for oxidation and reduction of the compounds are shown in Figure 10 and are in good agreement with values reported for other monomeric 10, 20-diarylporphyrinphosphonates diesters where the values of $E_{1/2}$ are linearly related to the Hammett substituent constants of the diethoxyphosphoryl groups, thus indicating that same redox process occurs throughout the series (Figure S49).[56]

Thus, no tetramer formation was detected by electrochemistry at room temperature in the solution of **Zn10** in either CH_2Cl_2 or PhCN, indicating a low stability of this species in the presence of the TBAP supporting electrolyte.

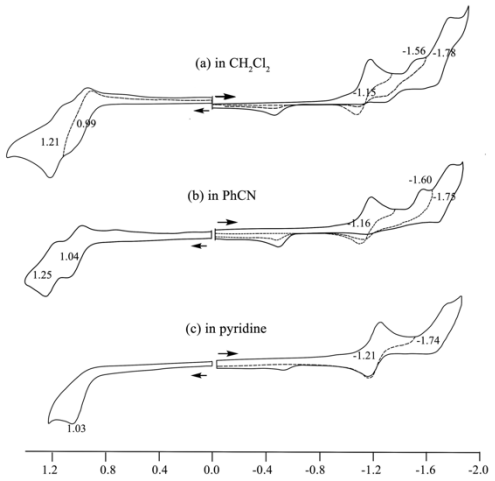

Fig. 11 Cyclic voltammograms of Zn10 in (a) CH_2Cl_2, (b) PhCN and (c) pyridine containing 0.1 M TBAP at a scan rate of 0.10 V/s.

Experimental Section

Materials

[10-(Diethoxyphosphoryl)-5,15-diphenylporphyrinato(2–)]zinc **(Zn5)**, [10-(dibuthoxyphosphoryl)-5,15-diphenylporphyrinato(2–)]zinc **(Zn6)**, [10-(diethoxyphosphoryl)-5,15-bis(4'-cyanophenyl)porphyrina-to(2–)]zinc **(Zn7)**, [10-(diethoxyphosphoryl)-5,15-bis(4'-tolyl)porphyrinato(2–)]zinc **(Zn8)**, [10-(diethoxyphosphoryl)-5,15-bis(4'-methoxyphenyl)-porphyrinato(2–)]zinc **(Zn9)**, {10-(diethoxyphosphoryl)-5,15-bis[(4'-(methoxycarbonyl)phenyl]-porphyrinato(2–)}zinc **(Zn10)**, {10-(dibuthoxyphosphoryl)-5,15-bis[(4'-(methoxycarbonyl)-phenyl]porphyrinato(2–)}zinc **(Zn11)** were prepared according to literature procedures.[45]

Dichloromethane (CH_2Cl_2, ≥99.8%), pyridine (Py, ≥99.9%) and tetra-*n*-butylammonium perchlorate (TBAP, ≥99.0%) were purchased from Sigma-Aldrich Co. and used as received. Benzonitrile (PhCN) was distilled over P_2O_5 under vacuum prior to use.

Instrumentation

^{1}H and ^{31}P NMR spectra were acquired on a Bruker Avance III 600 MHz spectrometer. Chemical shifts are expressed in parts per million (ppm), referenced on the δ scale by using residual non-deuterated solvent signals as an internal standard for ^{1}H

NMR spectroscopy and an external phosphonic acid (H_3PO_4) signal for ^{31}P NMR spectroscopy. Ground-state electronic absorption (UV-Vis spectra) were measured with a Cary 100 sp**ectroph**otometer in quartz cells with 1 mm and 1 cm optical path lengths in the 250-800 nm spectral region. Variable temperature UV-Vis spectra were recorded with a Thermo Evolution 210 spectrometer equipped with a Peltier thermostatting accessory. The spectra were recorded using quartz cells with a 1 cm optical path in the region of 450-650 nm. MALDI-TOF mass spectra were obtained on a Bruker Ultraflex II LRF 2000 mass spectrometer in positive ion mode with a dithranol matrix. Accurate mass measurements (HRMS) were made on a THERMO LTQ Orbitrap XL equipped with an electrospray ionization (ESI) source in positive mode unless otherwise stated. Solutions in $CHCl_3$/methanol (1:1) were used for the analysis. IR spectra were recorded on a FT-IR Nexus (Nicolet) spectrophotometer. A universal micro-ATR sampling accessory (Pike) was used in order to obtain IR spectra of solid samples.

All of the utilized spectrometers except for the Nexus (Nicolet) spectrophotometer and the Bruker Avance III 600 MHz were available at the "Pôle Chimie Moléculaire", the technological platform for chemical analysis and molecular synthesis (http://www.wpcm.fr) which relies on the Institute of the Molecular Chemistry of the University of Burgundy and WelienceTM, a Burgundy University private subsidiary.

Cyclic voltammetry was carried out at 298K using an EG&G Princeton Applied Research (PAR) 173 potentiostat/galvanostat. A homemade three-electrode cell was used for cyclic voltammetric measurements and consisted of a glassy carbon working electrode, a platinum counter electrode and a homemade saturated calomel reference electrode (SCE). The SCE was separated from the bulk of the solution by a fritted glass bridge of low porosity, which contained the solvent/supporting electrolyte mixture.

X-ray crystallographic analysis

Crystals of complexes **Zn5**–**Zn9** suitable for single crystal X-ray analysis were grown by a slow diffusion of hexane in 10^{-3} M solutions of the porphyrins in a $CHCl_3$/MeOH mixture (3% MeOH). The SCXRD experiment and refinement data are detailed in Supporting Information. CCDC-1844989 (**Zn5**), 1844992 (**Zn6**), 1844991 (**Zn7**), 1844990 (**Zn8**) and 1844993 (**Zn9**) contain the supplementary crystallographic information for this paper. These data can be obtained free of charge from the Cambridge Crystallographic Data Centre via www.ccdc.cam.ac.uk/data_request/cif.

Powder XRD experiments were carried out on a D8 Advance Diffractometer (Bruker AXS, Karlsruhe, Germany) with a goniometer radius 217.5 mm, Göbel Mirror parallel-beam optics, 2° Sollers slits and 0.2 mm receiving slit. PXRD patterns from 3° to 45° 2θ were recorded at room temperature using CuKα radiation (1.5418 Å) under the following measurement conditions: tube voltage of 40 kV, tube current of 40 mA, step scan mode with a step size 0.02° 2θ and counting time of 2.5 s/step. The samples were analyzed without being crushed. The phase purity of the polycrystalline samples was established for all complexes **Zn5**–**Zn9** and the experimental data are presented in Supporting Information (Figures S44-S48).

The X-ray measurements were performed using shared experimental facilities supported by IGIC RAS state assignment.

Calculation of average size of the Zn10 associates

To calculate the average number of molecules for associates of the **Zn10** complex in toluene at room temperature, UV-vis spectra were measured over a porphyrin concentration range of 5 x 10^{-3} to 5 x 10^{-6} M. The calculations were performed using absorption values of the Q bands at 544 and 571 nm according to equation 1)[54] where *n* is the number of chromophore molecules in the accociate, C_0 is the total concentration of the complex and K is the equilibrium constant.

$$\lg\left[C_0 \cdot \left(1-\frac{\varepsilon_{eff}}{\varepsilon_m}\right)\right] = \lg(n \cdot K) + n \cdot \lg\left[C_0 \cdot \left(\frac{\varepsilon_{eff}}{\varepsilon_m}\right)\right] \quad (1)$$

The average number of molecules in the associates was found by plotting the value $\lg\left[C_o(1-\varepsilon_{eff}/\varepsilon_m)\right]$ with $\lg\left[C_o(\varepsilon_{eff}/\varepsilon_m)\right]$ (Figure S43). Straight lines were obtained for both Q-bands with slopes close to 2 (1.822 and 2.106).

Conclusions

Self-assembly of seven 10-(dialkoxyphosphoryl)-5,15-diarylporphyrins (**Zn5**–**Zn11**) containing different substituents at the phosphoryl and aryl groups were investigated. Single crystals of five complexes (**Zn5**–**Zn9**) were grown under the same conditions and analyzed by X-ray structural analysis. A self-assembly of the porphyrin molecules through weak coordinative bonding of the phosphoryl group from one porphyrin to the zinc atom of the partner molecule is observed in crystals of all studied compounds. The geometries of the macrocycles are similar and the central zinc atom adopts a distorted tetragonal pyramidal environment in these crystals. However, the complexes **Zn5**–**Zn7** display a 1D polymeric structure while the complexes **Zn8** and **Zn9** exist as discrete cyclotetramers. The cyclotetramers were not earlier reported for (dialkoxyphosphoryl)porphyrins. All crystals are close-packed and there is not any solvent molecule occluded in the lattices. Thus, organization of the 10-(dialkoxyphosphoryl)porphyrins in the crystals is dependent upon the nature of the non-coordinating substituents on the macrocycle. The size of the substituents at the aryl group appears to be critical in determining organization of the porphyrin molecules in the crystals whereas electronic effects are less important. Porphyrins bearing bulky aryl groups tend to favor the formation of discrete tetrameric complexes.

Steric effects of substituents on the aryl and phosphonate groups also determine the mutual arrangement of polymeric chains of **Zn5**–**Zn7**. In the crystals of **Zn5**, the polymer chains are connected through CH–π interactions between the *para*-hydrogen atom of the phenyl substituent and delocalized

electron density of the tetrapyrrolic macrocycle. In the crystals of **Zn6** and **Zn7**, which consist of more bulky porphyrin molecules, the neighbouring polymer chains interact through short π–π contacts of neighbouring porphyrin macrocycles.
Self-assembly is also observed over a large temperature range (223 K–323 K) in toluene and chloroform solutions of **Zn5–Zn11.** Unfortunately, the associates exhibit a dynamic behavior that complicates their structural characterization. Nevertheless, the tetramer **$[Zn10]_4$** was unambiguously characterized by ^{1}H NMR spectroscopy in both toluene and chloroform solutions at 223 K. To our knowledge, this is the largest porphyrin associate ever formed through metal–oxygen coordinative bonding to be characterized in solution. As expected, the structure for associated **Zn10** in toluene and chloroform is concentration dependent. When solutions of this complex in toluene were diluted from 10^{-3} M to 10^{-5} M, the average number of molecules in the aggregate decreased to about 2. Taken altogether, the data in the current study demonstrates that (dialkoxyphosphoryl)porphyrins are useful model compounds to gain deeper insights into the self-assembly of tetrapyrroles which are widely observed in living matter.

Conflicts of interest

There are no conflicts to declare.

Acknowledgements

This work was supported by the Centre National de la Recherche Scientifique (CNRS), the Russian Academy of Sciences (RAS), FANO, Russian Foundation for Basic Research (grant number 17-53-16028) and the Robert A. Welch Foundation (KMK grant E-680). Work was carried out in the framework of the International Associated French–Russian Laboratory of Macrocyclic Systems and Related Materials (LAMREM) of CNRS. The authors thank Pr. R. Guilard, Dr. M. Volostnykh and Dr. Zhingpiing Ou for their helpful comments on this manuscript. The authors also thank J. Michalak for the optimization of the synthetic procedures for the preparation of (diethoxyphosphoryl)porphyrins.

References

1. J.-M. Lehn, *Supramolecular Chemistry: Concept and Perspectives.* , VCH, Weinheim, Germany, **1995**.
2. J. W. Steed and J. L. Atwood. *Supramolecular chemistry, 2nd Edition*, John Wiley and Sons, Blackwell, **2009**.
3. J. A. A. W. Elemans, R. van Hameren, R. J. M. Nolte and A. E. Rowan, *Adv. Mater.*, **2006**, *18*, 1251-1266.
4. Q. Zha, X. Rui, T. WeiandY. Xie, *CrystEngComm*, **2014**, *16*, 7371-7384.
5. Q. Zha, C. Ding, X. RuiandY. Xie, *Cryst. Growth Des.*, **2013**, *13*, 4583-4590.
6. X. Rui, Q.-Z. Zha, T.-T. WeiandY.-S. Xie, *Inorg. Chem. Commun.*, **2014**, *48*, 111-113.
7. T. S. Balaban, in *Handbook of Porphyrin Science*, eds. K. M. Kadish, K. M. Smith and R. Guilard, World Scientific, Singapore, 2010, vol. 1, ch. 3, pp. 221-306.
8. M. Morisue and Y. Kobuke, in *Handbook of Porphyrin Science*, eds. K. M. Kadish, K. M. Smith and R. Guilard, World Scientific, Singapore, 2014, vol. 32, ch. 166, pp. 1-126.
9. J. Deisenhofer, O. Epp, K. Miki, R. Huber and H. Michel, *J. Mol. Biol.*, **1984**, *180*, 385-398.
10. P. Jordan, P. Fromme, H. T. Witt, O. Klukas, W. Saenger and N. Krauss, *Nature*, **2001**, *411*, 909-917.
11. J.-C. Chambron, V. Heitz and J.-P. Sauvage, in *The Porphyrin Handbook*, eds. K. M. Kadish and K. M. Smith,R. Guilard, Academic Press, San Diego, 2000, vol. 6, pp. 1-42.
12. J. Wojaczyński and L. Latos-Grażyński, *Coord. Chem. Rev.*, **2000**, *204*, 113-171.
13. P. D. Harvey, in *The Porphyrin Handbook*, eds. K. M. Kadish, K. M. Smith and R. Guilard, Academic Press, San Diego, 2003, vol. 18, pp. 63-250.
14. I. Beletskaya, V. S. Tyurin, A. Y. Tsivadze, R. Guilard and C. Stern, *Chem. Rev.*, **2009**, *109*, 1659-1713.
15. C. M. Drain, A. Varotto and I. Radivojevic, *Chem. Rev.*, **2009**, *109*, 1630-1658.
16. P. D. Harvey, C. Stern and R. Guilard, in *Handbook of Porphyrin Science* eds. K. M. Kadish, K. M. Smith and R. Guilard, World Scientific Publishing, Singapore, 2011, vol. 11, pp. 1-180.
17. A. G. Bessmertnykh-Lemeune, C. Stern, R. Guilard, Y. Y. Enakieva, Y. G. Gorbunova, A. Y. Tsivadze and S. E. Nefedov, in *Supramolecular Systems: Chemistry, Types and Applications*, ed. C. Pena, Nova Science Publishers, 2016, pp. 213-278.
18. Y. Kobuke, in *Struct. Bond.*, ed. E. Alessio, Springer, Berlin, Heidelberg, 2006, pp. 49-104.
19. A. Satake and Y. Kobuke, *Tetrahedron*, **2005**, *61*, 13-41.
20. H. M. Goff, E. T. Shimomura, Y. J. Lee and W. R. Scheidt, *Inorg. Chem.*, **1984**, *23*, 315-321.
21. G. M. Godziela, D. Tilotta and H. M. Goff, *Inorg. Chem.*, **1986**, *25*, 2142-2146.
22. A. L. Balch, B. C. Noll, S. M. Reid and E. P. Zovinka, *Inorg. Chem.*, **1993**, *32*, 2610-2611.
23. J. Wojaczynski and L. Latos-Grazynski, *Inorg. Chem.*, **1995**, *34*, 1054-1062.
24. J. Wojaczyński and L. Latos-Grażyński, *Inorg. Chem.*, **1996**, *35*, 4812-4818.
25. E. Deiters, V. Bulach, N. Kyritsakas and M. W. Hosseini, *New J. Chem.*, **2005**, *29*, 1508-1513.
26. Y. Matano, T. Shinokura, K. Matsumoto, H. Imahori and H. Nakano, *Chem. - Asian J.*, **2007**, *2*, 1417-1429.
27. T. S. Balaban, *Acc. Chem. Res.*, **2005**, *38*, 612-623.
28. H. Tamiaki and M. Kunieda, in *Handbook of Porphyrin Science*, eds. K. M. Kadish, K. M. Smith and R. Guilard, World Scientific, Singapore, 2011, vol. 11, pp. 223-290.
29. T. Miyatake and H. Tamiaki, *J. Photochem. Photobiol. C,* **2005**, *6*, 89-107.
30. T. S. Balaban, M. Linke-Schaetzel, A. D. Bhise, N. Vanthuyne, C. Roussel, C. E. Anson, G. Buth, A. Eichhöfer, K. Foster, G. Garab, H. Gliemann, R. Goddard, T. Javorfi, A. K. Powell, H. Rösner and T. Schimmel, *Chem. - Eur. J.*, **2005**, *11*, 2267-2275.
31. M. Ptaszek, Z. Yao, D. Savithri, P. D. Boyle and J. S. Lindsey, *Tetrahedron*, **2007**, *63*, 12629-12638.
32. T. Jochum, C. M. Reddy, A. Eichhöfer, G. Buth, J. Szmytkowski, H. Kalt, D. Moss and T. S. Balaban, *Proc. Natl. Acad. Sci. USA*, **2008**, *105*, 12736-12741.

33. Y. Matano, in *Main Group Strategies towards Functional Hybrid Materials*, John Wiley & Sons, 2017, pp. 265-293.
34. F. Atefi and D. P. Arnold, *J. Porphyrins Phthalocyanines*, **2008**, *12*, 801-831.
35. F. Atefi, J. C. McMurtrie, P. Turner, M. Duriska and D. P. Arnold, *Inorg. Chem.*, **2006**, *45*, 6479-6489.
36. F. Atefi, J. C. McMurtrie and D. P. Arnold, *Dalton Trans.*, **2007**, DOI: Doi 10.1039/B703589f, 2163-2170.
37. Y. Matano, K. Matsumoto, Y. Terasaka, H. Hotta, Y. Araki, O. Ito, M. Shiro, T. Sasamori, N. Tokitoh and H. Imahori, *Chem. - Eur. J.*, **2007**, *13*, 891-901.
38. E. V. Vinogradova, Y. Y. Enakieva, S. E. Nefedov, K. P. Birin, A. Y. Tsivadze, Y. G. Gorbunova, A. G. Bessmertnykh-Lemeune, C. Stern and R. Guilard, *Chem. - Eur. J.*, **2012**, *18*, 15092-15104.
39. Y. Y. Enakieva, M. V. Volostnykh, S. E. Nefedov, G. A. Kirakosyan, Y. G. Gorbunova, A. Y. Tsivadze, A. G. Bessmertnykh-Lemeune, C. Stern and R. Guilard, *Inorg. Chem.*, **2017**, *56*, 3055-3070.
40. Y. Y. Enakieva, A. G. Bessmertnykh, Y. G. Gorbunova, C. Stern, Y. Rousselin, A. Y. Tsivadze and R. Guilard, *Org. Lett.*, **2009**, *11*, 3842-3845.
41. A. A. Sinelshchikova, S. E. Nefedov, Y. Y. Enakieva, Y. G. Gorbunova, A. Y. Tsivadze, K. M. Kadish, P. Chen, A. Bessmertnykh-Lemeune, C. Stern and R. Guilard, *Inorg. Chem.*, **2013**, *52*, 999-1008.
42. R. I. Zubatyuk, A. A. Sinelshchikova, Y. Y. Enakieva, Y. G. Gorbunova, A. Y. Tsivadze, S. E. Nefedov, A. Bessmertnykh-Lemeune, R. Guilard and O. V. Shishkin, *CrystEngComm*, **2014**, *16*, 10428-10438.
43. A. Lemeune, A. Y. Mitrofanov, Y. Rousselin, C. Stern, R. Guilard, Y. Y. Enakieva, Y. G. Gorbunova and S. E. Nefedov, *Phosphorus Sulfur Silicon Relat. Elem.*, **2015**, *190*, 831-836.
44. K. M. Kadish, P. Chen, Y. Y. Enakieva, S. E. Nefedov, Y. G. Gorbunova, A. Y. Tsivadze, A. Bessmertnykh-Lemeune, C. Stern and R. Guilard, *J. Electroanal. Chem.*, **2011**, *656*, 61-71.
45. Y. Y. Enakieva, J. Michalak, I. A. Abdulaeva, M. V. Volostnykh, C. Stern, R. Guilard, A. G. Bessmertnykh-Lemeune, Y. G. Gorbunova, A. Y. Tsivadze and K. M. Kadish, *Eur. J. Org. Chem.*, **2016**, 4881-4892.
46. A. Mitrofanov, A. B. Lemeune, C. Stern, R. Guilard, N. Gulyukina and I. Beletskaya, *Synthesis*, **2012**, *44*, 3805-3810.
47. A. Tsuda, T. Nakamura, S. Sakamoto, K. Yamaguchi and A. Osuka, *Angew. Chem., Int. Ed.*, **2002**, *41*, 2817-2821.
48. K. Funatsu, T. Imamura, A. Ichimura and Y. Sasaki, *Inorg. Chem.*, **1998**, *37*, 1798-1804.
49. K. Fukushima, K. Funatsu, A. Ichimura, Y. Sasaki, M. Suzuki, T. Fujihara, K. Tsuge and T. Imamura, *Inorg. Chem.*, **2003**, *42*, 3187-3193.
50. T. S. Balaban, R. Goddard, M. Linke-Schaetzel and J.-M. Lehn, *J. Am. Chem. Soc.*, **2003**, *125*, 4233-4239.
51. A. Tsuda, S. Sakamoto, K. Yamaguchi and T. Aida, *J. Am. Chem. Soc.*, **2003**, *125*, 15722-15723.
52. Y. Kobuke and H. Miyaji, *J. Am. Chem. Soc.*, **1994**, *116*, 4111-4112.
53. N. N. Gerasimchuk, A. A. Mokhir and K. R. Rodgers, *Inorg. Chem.*, **1998**, *37*, 5641-5650.
54. N. Mataga, *Bull. Chem. Soc. Jpn.*, **1957**, *30*, 375-379.
55. Y. Fang, K. M. Kadish, P. Chen, Y. Gorbunova, Y. Enakieva, A. Tsivadze, A. Bessmertnykh-Lemeune and R. Guilard, *J. Porphyrins Phthalocyanines*, **2013**, *17*, 1035-1045.
56. X. Fang, X. Jiang, K. M. Kadish, S. E. Nefedov, G. A. Kirakosyan, Y. Y. Enakieva, Y. G. Gorbunova, A. Y. Tsivadze, C. Stern, A. Bessmertnykh-Lemeune and R. Guilard, *Inorg. Chem.*, **2019**, submitted.
57. Y. Fang, Y. G. Gorbunova, P. Chen, X. Jiang, M. Manowong, A. A. Sinelshchikova, Y. Y. Enakieva, A. G. Martynov, A. Y. Tsivadze, A. Bessmertnykh-Lemeune, C. Stern, R. Guilard and K. M. Kadish, *Inorg. Chem.*, **2015**, *54*, 3501-3512.
58. K. M. Kadish, E. Van Caemelbecke and G. Royal, in *The PorphyrinHandbook*, eds. K. M. Kadish, K. M. Smith and R. Guilard, Academic Press, San Diego, 2000, vol. 8, pp. 1-114.
59. K. M. Kadish, G. Royal, E. Van Caemelbecke and L. Gueletti, in *The Porphyrin Handbook*, eds. K. M. Kadish, K. M. Smith and R. Guilard, Academic Press, San Diego, 2000, vol. 9, pp. 1-219.